Solvent-free synthesis of tetrahydropyran alcohols over acid-modified clays

Sidorenko, Alexander Yu.; Kurban, Yu M.; Aho, Atte; Ihnatovich, Zh.V.; Kuznetsova, TF; Heinmaa, Ivo; Murzin, Dmitry; Agabekov, Vladimir E.

Published in:
Molecular Catalysis

DOI:
10.1016/j.mcat.2020.111306

Published: 01/01/2021

Document Version
Accepted author manuscript

Document License
CC BY-NC-ND

Solvent-free synthesis of tetrahydropyran alcohols over acid-modified clays

A.Yu. Sidorenko[1], Yu.M. Kurban[1], A. Aho[2], Zh.V. Ihnatovich[1], T.F. Kuznetsova[3], I. Heinmaa[4], D.Yu. Murzin[2], V.E. Agabekov[1]

1 - Institute of Chemistry of New Materials of NAS of Belarus, 220141, Skaryna str, 36, Minsk, Belarus

2 - Åbo Akademi University, 20500, Biskopsgatan 8, Åbo-Turku, Finland

3 - Institute of General and Inorganic Chemistry of NAS of Belarus, 220072, Surganov str, 9/1, Minsk, Belarus

4 - National Institute of Chemical Physics and Biophysics, 12618, Akadeemia tee 23, Tallinn, Estonia

Corresponding authors

Dr. A.Yu. Sidorenko

e-mail: Sidorenko@ichnm.by;

Ph:+375 17 268 63 08

Address: Institute of Chemistry of New Materials of National Academy of Sciences of Belarus, 220141, Skaryna str., 36, Minsk, Belarus

Professor Dr. D.Yu. Murzin

Åbo Akademi University

Biskopsgatan 8, 20500, Turku/Åbo, Finland

Ph: + 358 2 215 4985

e-mail: dmurzin@abo.fi

Graphical Abstract

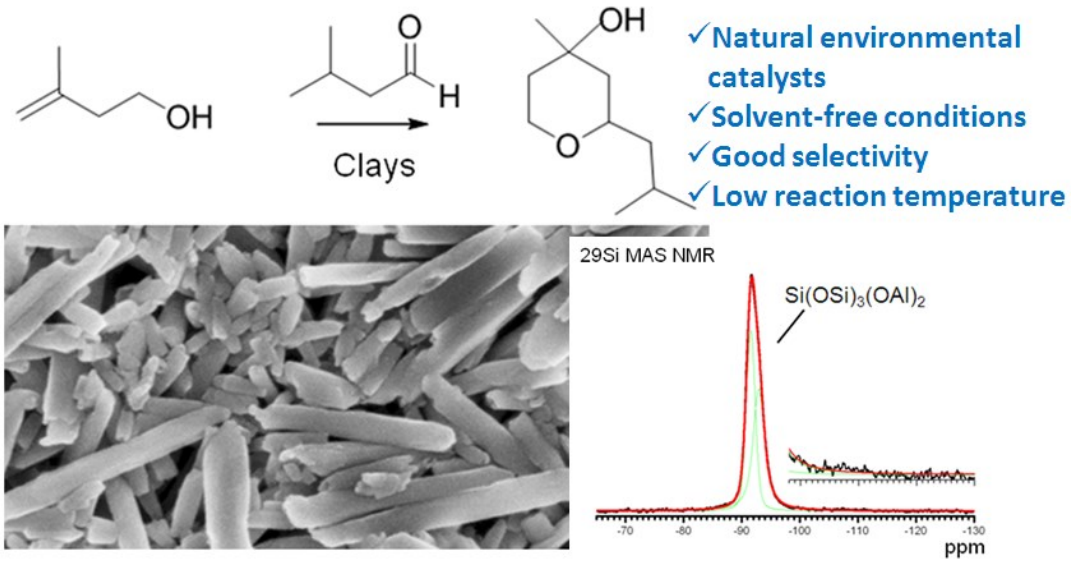

Abstract

A number of acid-modified clays (halloysite, montmorillonite, illite) were studied as catalysts for isoprenol cyclization with isovaleraldehyde to tetrahydropyranols used in perfumery as a mixture of *cis*- and *trans*- isomers. The main attention was paid to properties of halloysite nanotubes after treating them with 5% HCl at temperatures from 30 to 100°C. The catalysts were characterized by XRD, EDX, MAS NMR, SEM, and N_2 adsorption-desorption methods. The acid modification of halloysite allows an efficient increase of its acidity and specific surface area, while preserving morphology of nanotubes. On relatively weakly acidic clays, the formation of the target product occurs through a hemiacetal as a precursor. On the contrary, over strongly acidic resin Amberlyst-15, the yield of tetrahydropyranol was significantly lower because of a direct formation of tetrahydropyranols and dehydration by-products. The yield of tetrahydropyranol in the presence of clays was 65-72%, slightly increasing with an increase in their acidity. The selectivity towards the *cis*- isomer did not practically depend on the acid sites concentration in clays, decreasing slightly for the *trans*-isomer with decreasing acidity due to formation of the dehydration by-products. In general, acid-modified clays are promising catalysts for the preparation of tetrahydropyranols under mild conditions and in the absence of any solvent.

Keywords: Tetrahydropyranol; Isoprenol; Cyclization; Clays; Nanotubes, Acidity

1. Introduction

Many compounds with a tetrahydropyran (THP) structure have a variety of aromas being extensively used in the perfumery industry [1–3]. Tetrahydropyran derivatives also exhibit a wide range of biological activities (antiviral, anticancer, analgesic, etc.) and are active ingredients of some medicines [4, 5].

One of the main methods for the THP synthesis is Prins cyclization of unsaturated alcohols with carbonyl compounds [6, 7]. For example, 3-methylbut-3-en-1-ol 1 (isoprenol) or terpenoid (-) - isopulegol **5** can be used as starting reagents. Hemiacetal **2** is formed as an intermediate product of the reaction of alcohol **1** with aldehydes, being thereafter converted into tetrahydropyranol 3 and by-products 4 (Fig. 1). When isopulegol is used, 2*H*-chromene derivatives **6** and **7** are formed [3, 8–10].

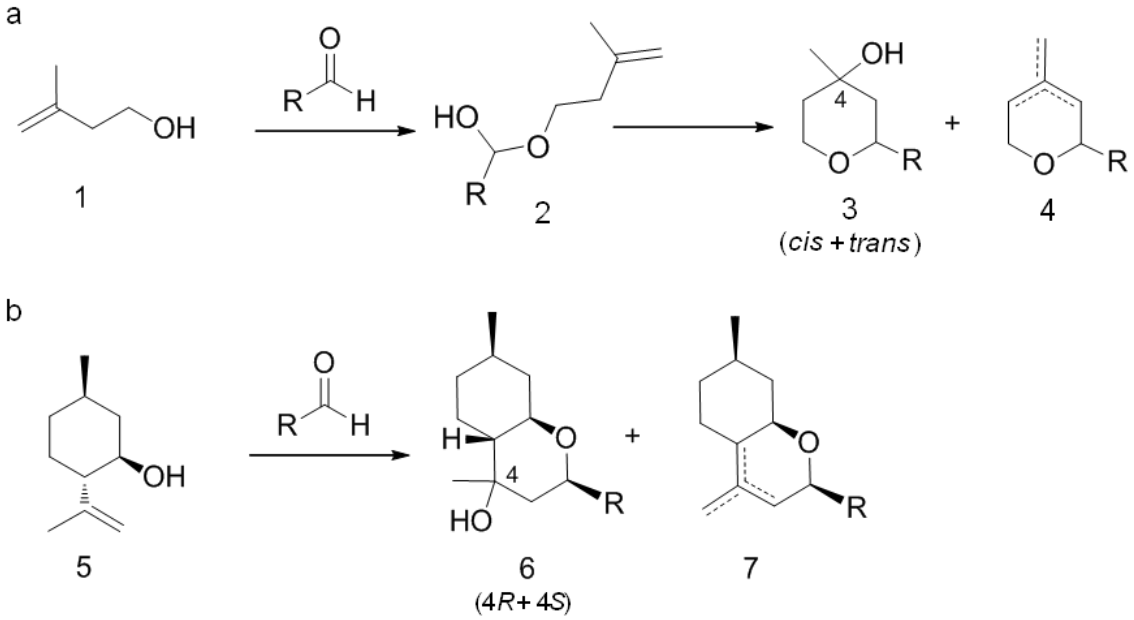

Fig. 1. Cyclization of aliphatic (a) and terpene (b) alcohols with aldehydes

Brønsted or Lewis acids can be used as traditional homogeneous catalysts for the Prins cyclization [6, 7, 11–13]. Recently, a number of novel catalytic systems (mesoporous silicates, oxides, zeolites, clays, etc.) with both types of acidity have been proposed for the preparation of tetrahydropyran alcohols [9, 10, 14–17]. For example, synthesis of tetrahydro-2*H*-pyranols **3** used in perfumery was carried out in the presence of *p*-TSA, MoO_3, and Fe supported on silica [3, 8, 18], smectite clays [16], and Amberlyst-15 resin [19].

Clays are effective and environmentally friendly catalysts for a number of organic reactions, including the Prins cyclization [20, 21]. One of the effective methods of increasing the catalytic and adsorption activity of clays (which are predominantly layered aluminosilicates) is their acid treatment [22, 23]. Such method leads to an increase in the concentration of H^+ on their surface due to ion exchange and washing out the structural ions (Al, Fe, Mg, etc.) [23]. For such processing, montmorillonite clays are most often used, because the resulting solids have a relatively high (200–300 m^2/g) specific surface area [23].

The clay mineral halloysite is a very promising starting material for the design of novel catalytic systems [24, 25]. Its layer is a combination of tetrahedral Si–O and octahedral Al–O sheets, which are bent into rolls and form nanosized multilayer tubes [26]. The image and crystal structure of this material are shown in Fig. SI (Supplementary information). Halloysite nanotubes (HNT), after their functionalization, possess catalytic activity in various reactions, for example, esterification, hydrocracking, cross-coupling, Fischer-Tropsch, etc. [27–30].

The authors have recently shown that acid-modified halloysite nanotubes are highly selective and stable catalysts for isopulegol **5** condensation with carbonyl compounds (Fig. 1b). In the presence of HNT the yield of octahydro-2*H*-chromenols **6** is up to 94% at a 4*R*/4*S* stereoisomer ratio of up to 14.5, which is higher than on other catalysts types [31]. It was assumed that the selective formation of the 4*R*-isomer on halloysite is due to generation of an intermediate on weak acid sites with a subsequent transfer of water molecules to it from the catalyst surface [31]. Addition of water to the reaction medium also leads to a slight increase in the selectivity to tetrahydropyran alcohols **2** [8, 32], whereas in the synthesis of tetrahydropyran amides (as 4*R*- and 4*S*- isomers), a quantitative inversion of stereoselectivity was observed with an increase in the water content [33].

The green chemistry principles among other measures include the use of renewable raw materials, non-toxic catalysts, conducting chemical reactions under mild conditions in the absence of a solvent to reduce the impact on the environment [34]. In the context of green chemistry development of efficient catalysts for the production of tetrahydropyran alcohols used in the perfumery industry is an important task.

The aim of this work is to study catalytic properties of the acid-modified clays with different structures (halloysite, montmorillonite, illite) in the cyclization reaction of unsaturated alcohols with aldehydes. The main attention is devoted to the study of halloysite nanotubes. Cyclization of isopenol **1** with isovaleraldehyde was chosen as a model reaction, because the corresponding tetrahydro-2*H*-pyranol **3** is a compound that is used as a mixture of *cis*- and *trans*-isomers in fragrance industry [2, 3].

2. Experimental

2.1. Preparation and characterization of the catalyst.

Halloysite nanotubes from the Dragon Mine (USA) were used as a starting material for preparation of the catalysts. The acid treatment of HNT was carried out with a 5% aqueous solution of hydrochloric acid at different (from 30 to 100 °C) temperatures. A weighed amount of halloysite (7–8 g) was introduced into a three-necked flask, the acid was added at the ratio of 5 ml of the solution per 1 g of clay (5 ml/g), heated to the required temperature and stirred for 3 h using a magnetic stirrer. Then the resulting solid phase was washed with distilled water until there were no Cl^- ions in the wash water (test with $AgNO_3$), dried at 105°C and kept in air at room temperature for at least 72 h to obtain an air-dry form of halloysite. For all studies, a fraction below 100 μm was used. Commercial acid-modified montmorillonites K-10 and K-30 (Germany), illite clay (Russia), and Amberlyst-15 resin were used for comparison. Illite was treated with 10% HCl at 90°C. The choice of the acid concentration was related to previous utilization of the same concentration for treatment of illite giving a material, which was extensively characterized by MAS NMR, EDX, and nitrogen physisorption [31].

The chemical composition of the samples was determined by energy-dispersive X-ray spectroscopy (EDX) using an electron microscope with a JEOL JCM-6000Plus chemical analysis system (Japan).

The parameters of the porous structure of halloysite were measured on an ASAP 2020 MP analyzer (Micromeritics). The samples (50 mg) were preliminarily evacuated (residual pressure 0.013 Pa) for 1 h at 200°C. The specific surface area was calculated using the Brunauer-Emmett-Teller (BET) method. The volume and the average diameter of the pores were determined using the Barrett – Joyner – Halenda method from the desorption branch of the isotherm [35].

X-ray phase analysis of HNT was carried out on a Dron-3 diffractometer (CuKα radiation, recording range of 2θ 5–50º). Images of halloysite nanotubes were obtained with a Zeiss Leo 1530 scanning electron microscope.

^{29}Si MAS NMR spectra of HNT were recorded on Bruker AVANCE-II spectrometer at 14.1T magnetic field using MAS probe for 4 mm od Si_3N_4 rotors. Single pulse spectra were accumulated with 4 μs pulse (4/9 π) excitation at 119.23 MHz with a repetition time of 120 s at 11 kHz sample spinning frequency. The chemical shifts are given in TMS scale. The fitting of the lines was carried out in Bruker TOPSPIN 3.1 program.

^{27}Al MAS NMR spectra were recorded at 208.49 MHz on Bruker AVANCE-III spectrometer with 18.8 T external field using Bruker MAS probe and 3.2 mm zirconia rotors. The spectra were collected by a single 0.6 μs pulse (π/18) excitation with a repetition time 1 s at 22 kHz sample

spinning frequency. The spectra are referenced to the frequency of $Al(NO_3)_3$ solution. The intensity in the spectra was normalized to the number of accumulations and to the sample mass.

Acidity of the modified halloysite nanotubes was determined by FTIR spectroscopy using pyridine as a probe molecule [36]. The samples were heated to 350°C for 1 h, then cooled to 100°C and saturated with pyridine for 30 min. To determine the concentration of weak, medium, and strong acid sites (a.s.), FTIR spectra were recorded at 100°C after desorption of pyridine at 150ºC, for medium and strong a.s. at 250°C, and for only strong ones at 350°C [37]. The Brønsted and Lewis a.s. were assigned to the characteristic absorption bands at 1545 cm^{-1} and 1450 cm^{-1}, respectively. Their amounts were determined using the Emeis extinction coefficients [38].

2.2. Reaction and analysis of products

All reagents purchased from Sigma-Aldrich, had at least 98.0% purity, and were used without further purification. Taking into account that, according to [8, 31, 32], the yield of tetrahydropyran derivatives increased in the presence of air-dry aluminosilicates or by adding water to the reaction mixture, the reactions were carried out without preliminary drying of the catalysts.

In a round-bottomed flask (25 ml) 0.8 g (9.1 mmol) of 3-methylbut-3-en-1-ol was introduced with an equivalent amount of isovaleraldehyde. After heating the mixture to 40°C, 0.8 g of the catalyst was added followed by starting a magnetic stirrer (400 rpm). Several experiments were also carried out using cyclohexane as a solvent, with the volume of the reaction mixture being 5.0 ml.

The composition of the reaction mixture was determined using a gas chromatograph Khromos GKh-1000 with a flame ionization detector and a Zebron ZB-5 capillary column (30m x 0.25mm x 0.25μm). Before chromatography, ethyl acetate was added to a sample of the reaction mixture and thoroughly shaken for 2-3 min to extract the products from the catalyst surface. As an internal standard, n-decade (99.9%) was used. The injector temperature was 250°C, the detector temperature was 260°C, and the programmed heating mode of the column was from 50 to 260°C at a rate of 10°C/min, followed by an isothermal mode at 260° C. The total analysis time was 30 min. A typical chromatogram of the reaction products is shown in Fig. S2. The initial reaction rate r_0 was defined as the amount of isoprenol converted in 1–5 min and related to the catalyst amount (mmol/(g·min)).

3. Results and Discussion

3.1. Physico-chemical properties of studied solids

The diffractogram of the initial halloysite (Fig. 2) exhibits a typical reflections set for this material with a characteristic peak at 7.3Å (001), which indicates the absence of water molecules between the nanotubes layers (7 Å-form) [39]. The diffraction pattern of HNT after their treatment

with 5% HCl at 50 and 100°C did not change (Fig. 2), confirming absence of any significant changes in their crystal structure.

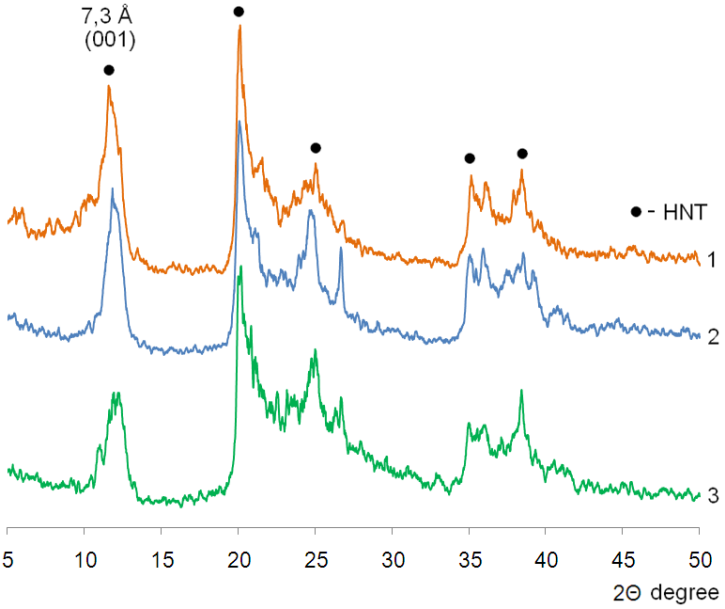

Fig. 2. X-ray diffraction patterns of the initial (1) and treated with HCl at 50 (2) and 100°C (3) halloysite

The chemical composition of the initial halloysite includes mainly alumina and silica oxides (Table 1). After treatment of HNT with hydrochloric acid at temperatures from 30 to 70°C, the content of the main components remained practically unchanged. In the case of modification at 90 and 100°C, a slight decrease in the content of Al_2O_3 and an increase in the amount of SiO_2 were observed (Table 1), reflecting a partial leaching of Al^{3+} ions from halloysite.

The nitrogen adsorption-desorption isotherms for the initial and modified samples of halloysite nanotubes (Fig. S3) correspond to type IV isotherm according to the IUPAC classification, characteristic of mesoporous materials, with a H3 shape hysteresis loop. The loop H3 is typical for slit-like pores formed by disordered non-rigid aggregates of lamellar or rod-like particles [40]. The specific surface area and the pore volume of the initial and treated at temperatures of 30 and 50°C halloysite nanotubes are practically the same (Table 1). A significant increase in S_{BET} (up to 123 m^2/g) occurred after modification of HNT at 100°C, when the removal of the largest amount of Al_2O_3 was observed. Note that the specific surface area of the commercial montmorillonites K-10 and K-30 is much higher than that of halloysite (Table 1).

Table 1. Chemical composition and porous structure of the studied aluminosilicates

Clay	Chemical composition, wt. %								Porous structure		
	Al_2O_3	SiO_2	FeO	Na_2O	MgO	K_2O	CaO	TiO_2	S_{BET}, m^2/g	V_{pore}, cm^3/g	D_{pore}, nm
Halloysite initial	44.9	53.9	0.6	0.1	0.1	-	0.4	0.3	60	0.22	15.7
Treated with 5% HCl at temperature, °C											
30	45.0	53.7	0.5	0.1	0.1	-	0.3	0.3	55	0.25	18.9
50	45.1	53.4	0.7	0.1	0.1	-	0.3	0.3	56	0.26	19.8
70	44.2	54.8	0.4	0.1	0.1	-	0.1	0.3	73	0.28	16.4
90	40.7	58.5	0.3	0.1	0.1	-	0.1	0.2	85	0.34	17.0
100	38.2	61.3	0.1	0.1	0.1	-	0.1	0.1	123	0.31	10.5
Illite*	19.8	64.4	6.4	0.1	1.7	5.7	0.1	1.9	146	0.28	8.1
K-10**	14.5	77.1	4.0	0.1	2.0	1.2	0.4	0.7	247	0.36	5.1
K-30	13.7	78.1	4.0	0.1	1.4	1.9	0.2	0.5	240	0.40	6.9

*The data from *[31] and **from [37]

The ^{29}Si MAS NMR spectrum of halloysite treated with HCl at 30°C (Fig. 3a) shows an intense peak at about -92 ppm, which belongs to the structural elements $Si(OSi)_3OAl_2$, where one silicon atom in the tetrahedral layer is surrounded by three Si atoms, as well as two Al atoms in the octahedral layer [31, 41, 42]. An asymmetric silicon resonance line at -92 ppm was fitted by two Gaussian peaks at -91.6 and -92.9 ppm. Such line shape can be attributed to the curvature of the layers of halloysite nanotubes. Note that the spectrum of the treated with HCl at 30°C halloysite (Fig. 3a) is identical to that for the starting material [31, 41, 42].

After acid modification of HNT at 50 and 70°C, practically no changes in the ^{29}Si MAS NMR spectra were observed (Fig. 3b,c). However, an increase in the acid treatment temperature to 90 – 100°C leads to appearance of two additional lines at ca. -102 and -111 ppm. (Fig. 3d,e). The peak at 102 ppm is assigned to $Si(OSi)_3OH$ units, in which one silicon atom is bound to three analogous ones and one -OH group [31, 41, 43]. A broad peak at -111 ppm corresponds to $Si(OSi)_4$ units (amorphous silica), which are formed upon crosslinking of $Si(OSi)_3OH$ fragments [31, 41, 43]. These structural elements are formed due to the breaking of Si-O-Al bonds between tetrahedral (Si-O) and octahedral (Al-O) layers of HNT [31, 41].

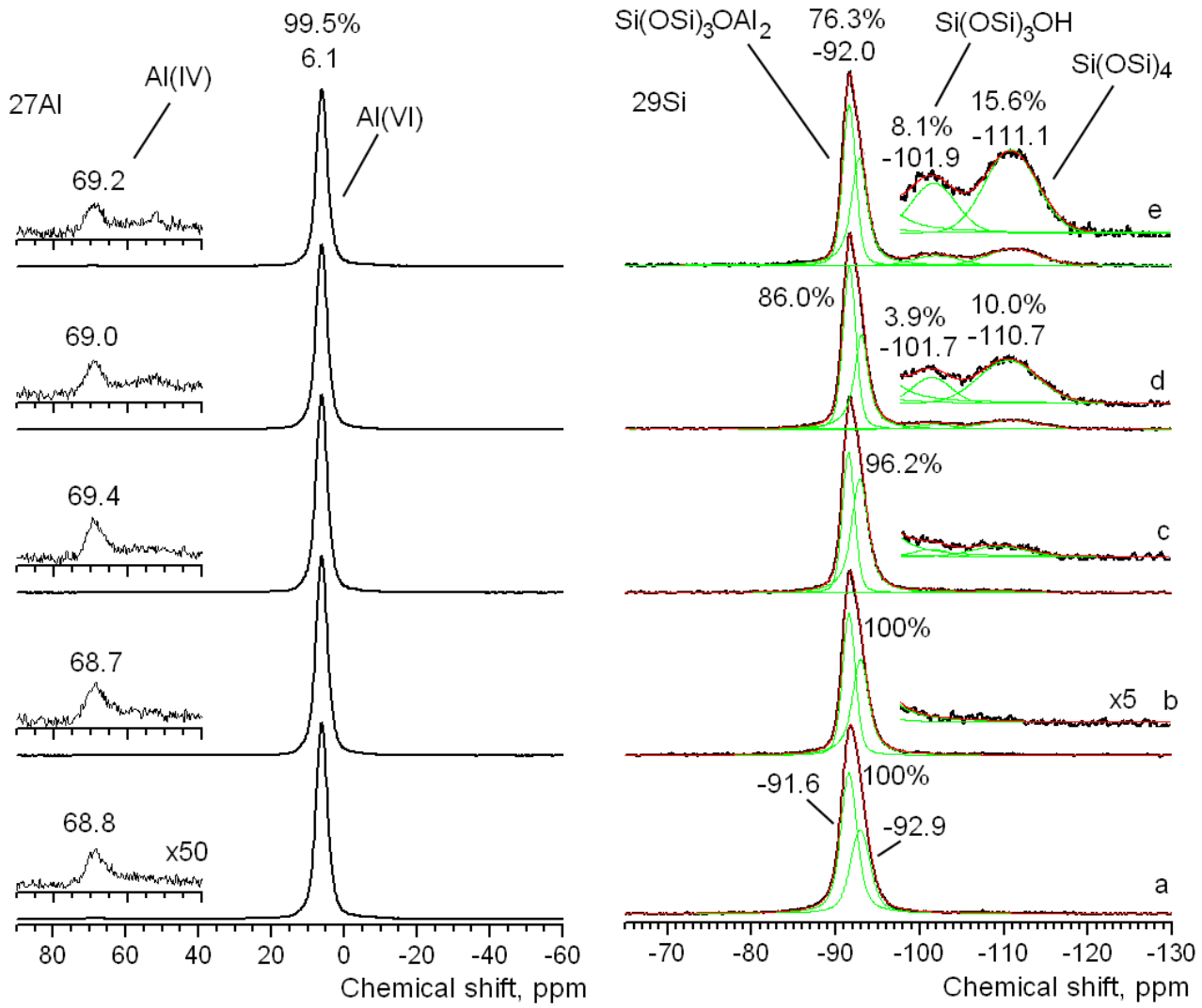

Fig. 3. ^{27}Al and ^{29}Si MAS NMR spectra of halloysite treated with 5% HCl at 30 (a), 50 (b), 70 (c), 90 (d) and 100°C (e)

Thus, after treatment of halloysite with 5% HCl at the temperature range from 30 to 70°C, there were no significant changes in its structure. As a result of the acid exposure at 90–100°C, a significant part (up to 23.7%) of the initial $Si(OSi)_3OAl_2$ units of halloysite nanotubes underwent destruction with formation of clays decomposition products (Fig. 3).

The ^{27}Al NMR spectra of halloysite (Fig.3) contain a characteristic line at 6.1 ppm, which refers to six-coordinated aluminum in the octahedral environment of this mineral [31, 42, 43]. In addition, very weak peaks (about 0.5%) are observed at 69 ppm., corresponding to four-coordinated Al atoms in tetrahedral layers of HNT [31, 42, 43]. Note that acid treatment of halloysite does not affect the distribution of aluminum atoms between its tetra- and octahedral layers.

Integrated line intensity at 6.1 ppm in the ^{27}Al MAS NMR spectra did not decrease after treatment of halloysite at temperatures up to 70°C (Fig. S4), which clearly indicates that the aluminum content in the samples does not change. A decrease in this signal was observed after HNT

modification at 90 and 100°C, which is fully consistent with the results of chemical analysis (Table 1).

It should be noted that the ^{29}Si and ^{27}Al MAS NMR spectra of commercial montmorillonites K-10, K-30 are described in detail in [37], whereas those for acid-treated illite are given in [31]. In the ^{29}Si MAS NMR spectra of these clays, in addition to the main peak at -92 ppm lines characteristic of acid-modified clays at -101 ($Si(OSi)_3OH$) and -111 ppm (amorphous silica) [31, 37] were also observed. It is important to note that 24% of Al^{3+} atoms in illite and *ca.* 20% in montmorillonites K-10 and K-30 are in the four-coordinated form due to the isomorphic substitution of Al^{3+} for Si^{4+} in the tetrahedral layers of these clays [31, 37], whereas such replacement was not observed in halloysite (Fig. 3).

Scanning electron microscopy (SEM) images of halloysite treated with 5% HCl at 30°C show characteristic nanosized tubes (Fig. 4a), which are morphologically identical to the original HNT of the Dragon Mine deposit [31, 41]. An increase in the acid modification temperature to 100°C did not lead to visible changes in the halloysite morphology (Fig. 4b). According to [31], significant destruction of halloysite nanotubes occurs when the content of structural units $Si(OSi)_3OAl_2$ in the acid-modified material according to ^{29}Si MAS NMR spectroscopy becomes less than 50%.

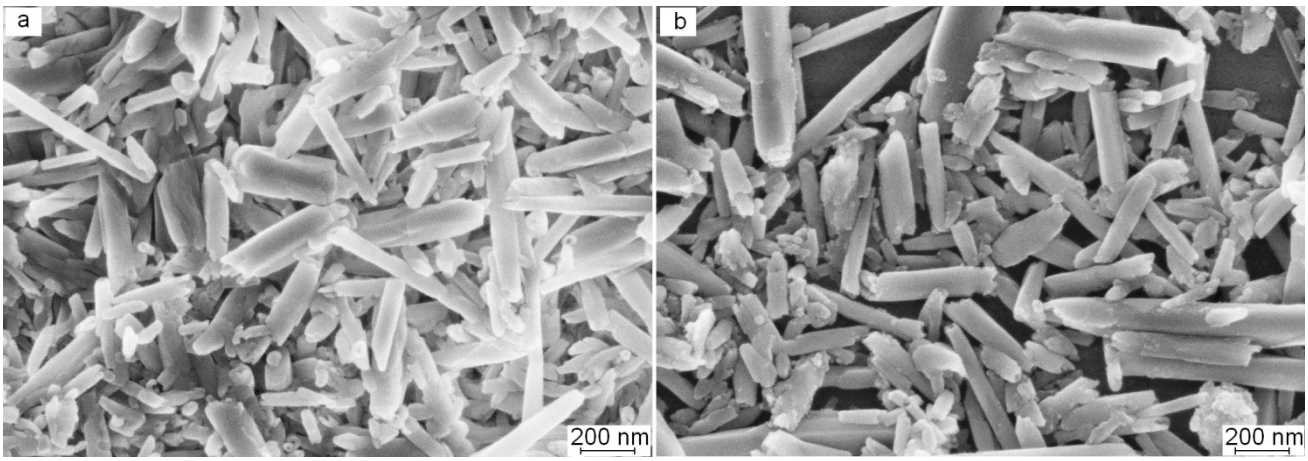

Fig. 4. SEM images of halloysite treated with 5% HCl at 30 (a) and 100°C (b)

Concentration of acid sites (a.s.) in the initial halloysite was 34 μmol/g and increased after its treatment with hydrochloric acid (Table 2). Thus, after the modification of HNT at 100°C, the content of a.s. increased to 55 μmol/g. Montmorillonites K-10 and K-30 are characterized by a significantly higher acidity (Table 2).

In the initial and modified with HCl at 30–50°C HNT, only weak and medium a.s. are present, whereas a higher treatment temperature led to the appearance of strong Lewis and Brønsted sites (Table 2). This may be because of an increase in the degree of cation exchange on the clay

surface. Note that the weak acid sites predominate in halloysite nanotubes and illite (Table 2). After the acid treatment of HNT the ratio of the weak (W) to the sum of the medium and strong (M + S) acid sites sharply decreased. Lewis acidity is dominant in almost all studied aluminosilicates (Table 2).

Table 2. Acidic properties of the investigated solids

Clay	Concentration of acid sites, μmol/g							L/B	$\frac{W}{M+S}$
	Brønsted (B)			Lewis (L)			Total		
	Weak (W)	Medium (M)	Strong (S)	Weak (W)	Medium (M)	Strong (S)			
Halloysite initial	12	1	0	17	4	0	34	1.6	5.8
Treated with 5% HCl at temperature, °C									
30	10	9	0	15	4	0	38	1.9	1.9
50	13	5	0	15	5	0	37	1.2	2.8
70	11	10	3	16	4	1	45	1.5	1.5
90	9	12	2	16	4	2	45	1.3	1.3
100	12	11	4	21	6	1	55	1.5	1.5
Illite	15	19	3	19	7	0	63	0.7	1.2
K-10*	15	26	7	35	14	7	104	1.2	0.9
K-30*	17	17	8	28	24	6	100	1.4	0.8

*The data from [37]

Differences in acidity of the studied clays can be explained by the specificities of their structure. Illite and montmorillonites are characterized by a partial isomorphic substitution of cations Al^{3+} for Si^{4+} in tetrahedral layers and metal cations of lower valency than Al^{3+} in octahedral layers. As a result, a negative charge arises on the surface of these minerals, which is compensated by exchangeable cations, including H^+ [20, 37]. In montmorillonites, these ions are located both on the particles surface and in the interlayer space, while for illite, they are present predominantly on the surface [20, 22, 37]. Thus, acidity of montmorillonites K-10 and K-30 is significantly higher than that of illite (Table 2).

In halloysite, the isomorphism phenomenon is absent, i.e. practically all Al^{3+} atoms are in the six coordinated states (Fig. 3), i.e. in octahedral layers, while Si^{4+} species occupy tetrahedral layers and therefore the total charge of layers is balanced [26, 31]. Subsequently acid sites in HNT should be located mainly only at the ends and defects of nanotubes, which determines their low concentration and strength (Table 2).

Thus, the acid treatment of halloysite nanotubes from the Dagon Mine deposit with a 5% HCl solution at temperatures from 30 to 100°C and at a relatively low ratio of the acid volume to the clay weight (5 ml/g) allows to increase the concentration and strength of acid sites, as well as the specific surface area, fully preserving the nanotubes morphology.

3.2. Activity of the studied catalysts

The main product of the isoprene **l** reaction with isovaleraldehyde without a solvent was tetrahydro-2*H*-pyranol **3** as *cis*- and *trans*-isomers (Table 3).

In the presence of initial halloysite, the conversion of alcohol **1** for 6 h was 73.0%, with a relatively low selectivity to tetrahydropyranols 3 (49.3%). Hemiacetal **2** and dehydration products **4** were also present in the reaction mixture (Table 3).

Treatment of halloysite nanotubes with HCl resulted in a significant increase in both the initial rate of isoprenol consumption (r_0) and selectivity to the desired product **3** (Table 3). The yield of tetrahydropyranol on modified HNT at 99.0% isoprenol conversion was practically the same (65–67%). A somewhat higher selectivity to **3** was observed in the presence of illite (70.2%) and montmorillonites K-10 and K-30 (*ca.* 71%), while the yield of by-products **4** decreased (Table 3). The highest value of r_0 was observed in the presence of Amberlyst-15 resin, while the yield of tetrahydropyranols was lower (63.0%) than on clays (Table 3).

Table 3. Selectivity* in the reaction of isoprenol with valeraldehyde at 40°C in solvent free conditions

Catalyst	r_0, mmol/g·min	Time, min	Selectivity, mol. %					*Cis*/*trans* ratio
			2	3	*cis*-3	*trans*-3	4	
Halloysite initial**	0.44	360	19.9	49.3	37.0	12.3	8.9	3.0
Treated with 5% HCl at temperature, °C								
30	0.57	360	0	65.1	47.5	17.6	14.0	2.7
50	0.58	360	0	64.8	47.1	17.7	14.2	2.7
70	0.65	300	0	66.5	48.7	17.8	12.8	2.7
90	0.67	300	0	67.4	49.2	18.2	12.9	2.7
100	0.69	300	0	66.4	47.7	18.7	15.0	2.6
Illite	0.72	300	0	70.2	48.7	21.5	10.1	2.3
K-30	0.81	180	0	71.2	47.3	23.9	7.2	2.0
K-10	0.91	120	0	71.8	47.3	24.5	8.9	1.9
Amberlyst-15	2.9	10	0	63.0	43.0	20.0	29.7	2.2

*At 99% of isoprenol conversion; **Conversion was 73% for 6 h

In the presence of all studied catalysts, the *cis*-isomer of tetrahydropyranol **3** prevailed in the reaction mixture, the content of which in the presence of modified halloysite, illite, and montmorillonites was practically the same (Table 3). The highest selectivity for the *trans*-isomer was

observed in the presence of clays K-10 and K-30. Therefore, the *cis*/*trans* ratio on these catalysts was somewhat lower than on halloysite nanotubes (Table 3). Note that a mixture of both isomers of tetrahydropyranol is used as a fragrant compound in perfumery [3]. Moreover, according to [44], the *cis*-isomers of tetrahydropyran compounds have a more fine aroma.

The initial reaction rate increased with an increase in the concentration of acid sites in the aluminosilicate catalysts (Fig.5a). At the same time, a slight increase in the selectivity for tetrahydropyranols **3** was also observed (Fig.5b). Thus, a relatively high acidity of the catalyst favors formation of these compounds. Since acid sites in halloysite are located mainly at the ends and defects of nanotubes, the isoprenol cyclization with isovaleraldehyde in this case should occur on the external surface of the nanotubes. In montmorillonites, a.s. are present both on the surface and in the interlayer space [20, 37]. Taking into account an increase in the initial reaction rate when using more acidic K-10 and K-30 (Fig. 5a), formation of products can also occur in the pores of these catalysts. Note that, according to [8–10, 16], the Prins cyclization effectively proceeds in the presence of mesoporous materials.

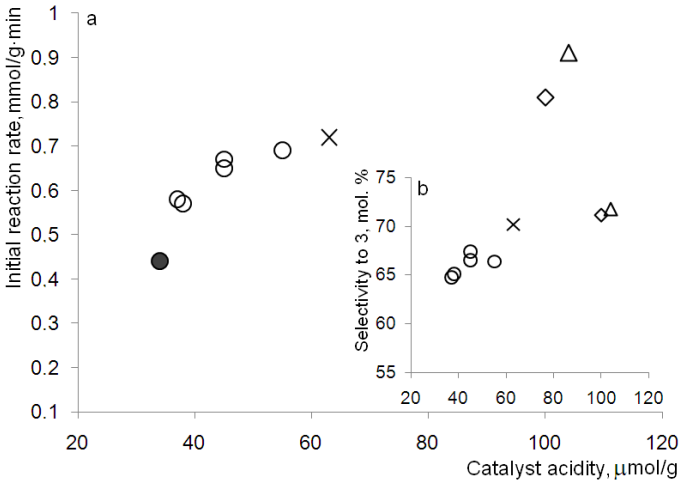

Fig. 5. Initial reaction rates (a) and selectivity to tetrahydropyranols at 99% isoprenol conversion (b) in solvent free conditions as a function of catalyst acidity
(● - initial and ○ - modified HNT; X - illite Δ - K-10; ◊ - K-30)

Note that after reaching *ca.* 50% isoprenol conversion, the reaction mixture became viscous solidifying thereafter, which made analysis of the concentration profiles very challenging. For example, 99% of isoprenol conversion was observed after 5 h even if the initial reaction rates for several catalysts were different (Table 3), clearly indicating that in a number of cases complete conversion of the alcohol was achieved in a shorter time. Therefore, for a detailed study of the selectivity dependence on the alcohol **1** conversion, cyclization was carried out in cyclohexane as a solvent.

The main product of the reaction in cyclohexane on modified halloysite at isoprenol conversion below 70% was hemiacetal **2** (Fig. 6a). With a further increase in the alcohol conversion, selectivity to the product **2** began to decrease sharply, increasing for tetrahydropyran compounds **3** and **4**. Such dependences indicate that formation of tetrahydropyranols 3 on halloysite nanotubes occurs mainly through the hemiacetal as an intermediate product. Note that, according to [16, 18, 32], formation of hemiacetals in the reactions of unsaturated alcohols with carbonyl compounds was observed in the presence of catalysts possessing both Lewis and Brønsted acidity. Moreover, a hemiacetal as the main product was observed on the weakly acidic $Fe(NO_3)_3/SiO_2$ [18], which is fully consistent with the results obtained in the current study on halloysite.

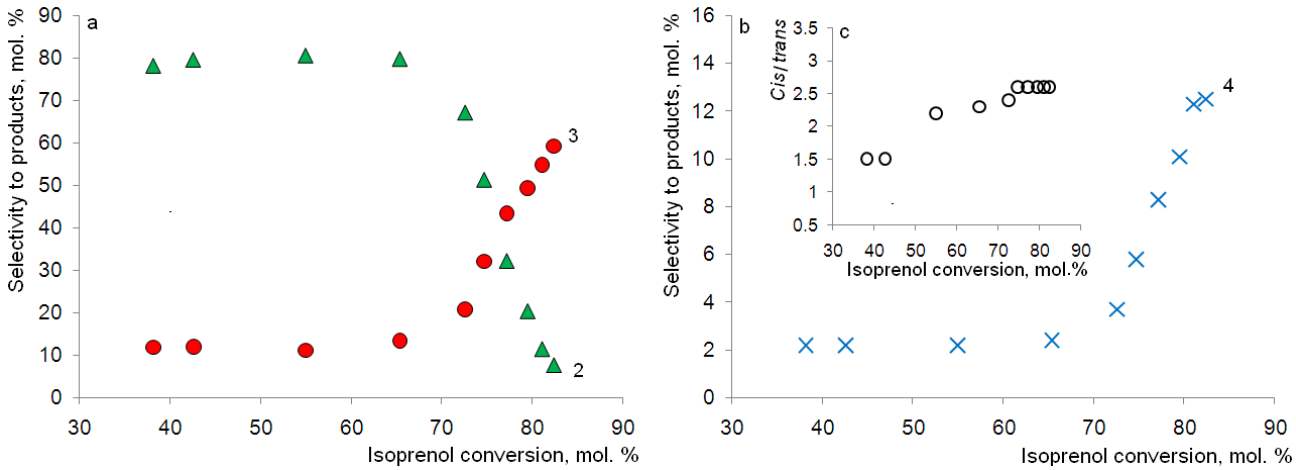

Fig. 6. Product selectivity (a, b) and *cis*/*trans* isomers ratio (c) as a function on the isoprenol conversion in cyclohexane over halloysite modified at 90°C

At 60% of isoprenol conversion, selectivity to hemiacetal **2** decreased from 80.1 to 50.2%, while selectivity to tetrahydropyranols **3** increased from 12.4 to 36.4% with an increase in the catalyst acidity from 45 to 104 μmol/g, respectively (Table 4). The highest selectivity to the product **3** (57.6%) and dehydration products 4 (21.0%) was observed in the presence of a strong Brønsted acid (Amberlyst-15). With an increase in the catalyst acidity, the initial rate of isoprenol consumption also increased (Table 4).

Table 4. The products selectivity * in the reaction of isoprenol with isovaleraldehyde at 40°C in cyclohexane

Catalyst	Acidity, μmol/g	r_0, mol/L·g·min	Time, min	Selectivity, mol. %			*Cis*/*trans* ratio
				2	3	4	
Halloysite**	45	0.17	45	80.1	12.4	2.3	2.3
Illite	63	0.22	15	77.4	13.9	2.0	2.1
K-10	104	0.29	10	50.2	36.4	3.0	1.9
Amberlyst-15***	-	1.1	2	16.4	57.6	21.0	2.2

*At 60% of isoprenol conversion 60%; **Treated with 5% HCl at 90°C; ***Total capacity ≥1.7 mol/l

Thus, in the presence of halloysite, illite, and montmorillonite catalysts, the intermediate step of the reaction is the condensation of isoprenol **1** and isovaleraldehyde into hemiacetal **2**, which, after consumption of more than 70% of **1**, undergoes cyclization to tetrahydropyranols **3** and tetrahydropyrans **4** (Fig. 7). In this case, selectivity to compound **2** at 60% isoprenol conversion sharply increases with a decrease in the catalyst acidity (Table 4), i.e. the reaction route through hemiacetal becomes predominant on weak acid sites. Similarly, isopulegol condensation with acetone to octahydrochromenols on halloysite proceeds through formation of an ester with isopulegol as an intermediate product [45].

Note that the shape of the selectivity curves for the reaction products from isoprenol conversion on halloysite (Fig. 6) and montmorillonite K-10 (Fig. S5) was practically the same, although selectivity to hemiacetal on K-10 was lower, due to its higher acidity. In the case of Amberlyst-15, compound **2** was formed in significantly smaller amount (Table 4, Fig. S6), which may indicate the direct formation of tetrahydropyranols **3** from the reagents on strong Brønsted a.s.

On the other hand, in the presence of a strong acidic Amberlyst-15, the highest yield of compounds **4** should be associated with deprotonation of ion **I-2**, which is formed directly from the reagents, and not through the hemiacetal.

In the presence of all studied catalysts, both selectivity to products **3** and **4** increased with an increase in isoprenol conversion (Fig. 6, S5,S6), which clearly indicates their formation in a parallel fashion. Moreover, these experimental data do not provide a solid evidence for dehydration of tetrahydropyranols to products **4**.

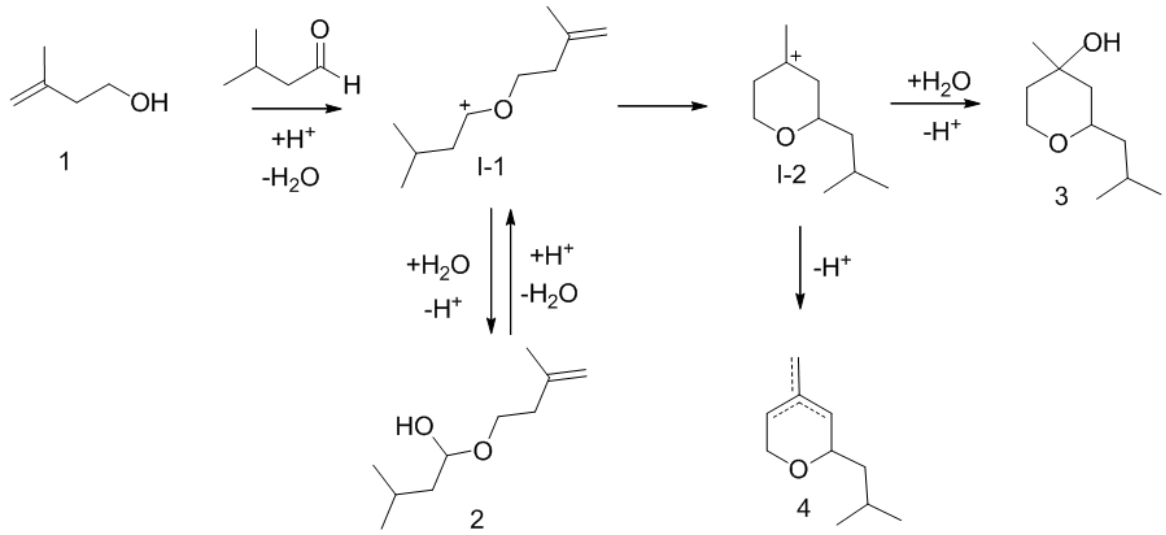

Fig. 7. Mechanism of isoprenol cyclization with isovaleraldehyde

In the absence of a substituent in the fourth position of the THP ring, complete *cis*-selectivity in formation of tetrahydropyranols was observed [46]. According to the Alder's calculation model, this occurs because of the effective overlap of the empty *p*-orbital of the carbocationic center, in which the hydrogen atom is pseudo-axial, with coplanar σ-orbitals of carbon atoms and a pair of non-bonding oxygen electrons, which leads to an addition of the nucleophile to the equatorial position [47].

The presence of a methyl group at C_4 of THP leads to formation of both diastereomers of tetrahydropyranol with an excess of the *cis*-isomer [8, 16, 18]. The predominant *cis*-selectivity towards tetrahydropyranol **3** was also observed in the current work. Moreover, the yield of *cis*-isomer was practically the same for all studied aluminosilicate catalysts (Table 3). The lowest selectivity for the *trans*-isomer **3** was observed on the modified halloysite, while the yield of dehydration products increased (Table 3). For this reason, there is a slight decrease in the overall selectivity for product **3** on HNT. It can be assumed that on weak a.s. of halloysite, after a partial deprotonation of the specific conformation of the adsorbed **I-2**, the latter is then converted into the *trans*-isomer of tetrahydropyranol.

Over HNT the *cis*/*trans* isomer ratio increases with an increase in alcohol **1** conversion to 70% and then remained practically unchanged (Fig. 6c). A similar dependence was observed on montmorillonite K-10 (Fig. S5), while on Amberlyst-15, the *cis*/*trans* ratio was practically independent of conversion (Fig. S6). A constant *cis*/*trans* value for halloysite nanotubes and K-10 was observed when formation of tetrahydropyranols occurs due to consumption of hemiacetal (Fig. 6), or directly from reagents on Amberlyst-15 (Fig. S6).

A lower *cis*/*trans* ratio during the reaction phase with predominant accumulation of the hemiacetal, can be explained by direct formation of tetrahydropyranols **3** from the reagents (Fig. 7). In this case, the conformations of the adsorbed intermediates **I-1**, **I-2** are somewhat more favorable for the *trans*-isomer formation.

After consumption of more than 70% of isoprenol, the hemiacetal starts to be transform into products **3** through species **I-1** and **I-2**, which can adsorb on the catalyst surface in a form which is more favorable for the *cis*-isomer formation, than during the initial reaction period. Similarly, to explain changes in stereoselectivity to the dialkylbenzenes hydrogenation products on conversion, a "rollover" mechanism was proposed, including the desorption-readsorption of the intermediates [48].

Comparison of the catalytic properties of various materials in the isoprenol cyclization with isovaleraldehyde is given in Table 5. Relatively low yields of tetrahydropyranols (up to 59%) were observed in the presence of sulfuric acid and p-TSA as homogeneous catalysts. The yields of these products can be increased by using heterogeneous counterparts. Thus, in the presence of Amberlyst-15 resin, the selectivity to product **3** increased to 67%, while on $FeCl_3/SiO_2$, it was 79.6% (Table 5).

According to [16], the yield of **3** on clay K-10 at 70°C was lower (61.0%) than in the present study at 40°C (71.8%). Comparable yields of tetrahydropyranols were observed over modified halloysite nanotubes and the illite clay. At the same time, the highest ratio of *cis*/*trans* isomers of compound **3** was observed on HNT (Table 5).

Table 5. Comparison of different catalysts in isoprenol cyclization with isovaleraldehyde

Catalyst	Temperature	Time, min	Selectivity, mol. %	*Cis*/*trans* ratio	Ref.
H_2SO_4*	70	-	55.0	-	32
p-TSA*	--//--	-	59.0	-	32
Amberlyst-15*	--//--	-	67.0	-	32
--//--	--//--	660	51.0		19
--//--	40	10	63.0	2.2	this work
$FeCl_3/SiO_2$	90	300	79.6	-	18
MoO_3/SiO_2	70	300	51.0	1.4	8
K-10	70	-	61.0	-	16
--//--	40	120	71.8	1.9	this work
Halloysite**	--//--	300	67.4	2.7	--//--
Illite**	--//--	300	70.2	2.3	--//--

*With 5% H_2O addition ** Treated with HCl at 90 °C

Thus, acid-modified halloysite, illite, and montmorillonite clays are promising catalysts for isoprenol cyclization with isovaleraldehyde, in the presence of which the selectivity for tetrahydropyranols can reach 72% at relatively low temperatures and in solvent-free conditions.

4. Conclusions

Acid-modified halloysite, montmorillonite and illite clays were studied as catalysts for the isoprenol cyclization with isovaleraldehyde to substituted tetrahydro-2*H*-pyran-4-ol, which is used in fragrance compositions as a mixture of *cis*- and *trans*- isomers.

A series of modified halloysite nanotubes (HNT) were obtained by treating the starting material with 5% HCl at temperatures ranging from 30 to 100°C. The materials were characterized by XRD, EDX, MAS NMR, SEM, and N_2 adsorption-desorption methods.

With an increase in the temperature of the HNT treatment from 30 to 100°C, their specific surface area and acidity increased from 60 to 123 m^2/g, and from 38 to 55 μmol/g, respectively. Exposure of halloysite to hydrochloric acid at 30–70°C did not lead practically to any changes in its crystal structure. Morphology of nanotubes was also completely preserved whereas at 100°C, 24% of the structural units ($Si(OSi)_3(OAl)_2$) were destroyed.

On modified clays with a relatively low acidity (38–104 μmol/g), generation of tetrahydro-2*H*-pyranol proceeds mainly with formation of the hemiacetal, while in the presence of a strong Brønsted acid (Amberlyst-15), the direct formation of this product from reagents prevails. At 99% conversion of isoprenol, selectivity to tetrahydropyranol increased from 65 to 72% with an increase in the catalyst acidity from 38 to 104 μmol/g, respectively. A slightly lower yield of the target product in the presence of weakly acid halloysite is due to the partial conversion of the hemiacetal into the side products – tetrahydropyrans.

Selectivity towards the *cis*-isomer of tetrahydropyranol did not depend on the acid sites concentration in the studied clays, while for the *trans*-isomer it decreased with decreasing acidity. This may be because of the partial deprotonation of the adsorbed form of the intermediate, which is responsible for the *trans*-isomer formation. The lowest yield of tetrahydropyranols (63%) was observed in the presence of Amberlyst-15 resin giving substantial amounts of dehydration products.

In general, acid-modified halloysite, illite, and montmorillonite clays can be considered as promising catalysts for cyclization of unsaturated alcohols with aldehydes at relatively low temperatures in the absence of any solvent.

Declaration of Competing Interest

The authors declare no conflict of interest.

Acknowledgments

This work is part of a Scientific Research Program funded by the National Academy of Sciences of Belarus (Grant No 4.1.16). I. H. was supported by the European Regional Development Fund (Grant No TK134).

References

1. H. Surburg, J. Panten, Common fragrance and flavor materials. Preparation, properties and uses. 5th Ed., WILEY-VCH Verlag GmbH & Co. KGaA, Weinheim, 2006.

2. F. Doro, N. Akeroyd, F. Schiet, A. Narula, The Prins Reaction in the fragrance industry: 100th Anniversary (1919-2019), *Angew. Chem. Int. Ed*., 2019, 22, 7174-7179.

3. A. Macedo, E.P. Wendler, A.A. Dos Santos, J. Zukerman-Schpector, E.R.T Tiekink, Solvent-free catalysed synthesis of tetrahydropyran odorants: the role of SiO_2/p-TSA catalyst on the Prins-cyclization reaction, *J. Braz. Chem. Soc*., 2010, 21, 1563–1571.

4. K.U. Sadek, R. A.H. Mekheimer, M. Abd-Elmonem, A. Abdel-Hameed, M.H. Elnagdi, Recent developments in the enantioselective synthesis of polyfunctionalized pyran and chromene derivatives. Tetrahedron: Asymmetry, 2017, 28, 1462–1485.

5. N. Thomas, S.M. Zacharian, Pharmacological activities of chromene derivatives: An overview. *Asian J. Pharm. Clin. Res*. 2013, 6, 11–15.

6. C. Olier, M. Kaafarani, S. Gastaldi, M. Bertrand. Synthesis of tetrahydropyrans and related heterocycles via prins cyclization; extension to aza-prins cyclization, Tetrahedron, 2010, 66, 413–445

7. X. Han, G. Peh, P.E. Floreancig, Prins-type cyclization reactions in natural product synthesis, Eur. J. Org. Chem., 2013, 1193–1208.

8. L. Sekerová, E. Vyskočilová, L. Červený, Prins cyclization of isoprenol with various aldehydes using MoO_3/SiO_2 as a catalyst, *Reac. Kinet. Mech. Cat.*, 2017, 121, 83–95.

9. M. Stekrova, P. Mäki-Arvela, N. Kumar, E. Behravesh, A. Aho, Q. Balme, K.P. Volcho, N.F. Salakhutdinov, D.Yu. Murzin, Prins cyclization: Synthesis of compounds with tetrahydropyran moiety over heterogeneous catalysts, J. Mol. Catal. A: Chem. 410 (2015) 260–270.

10. A.Yu. Sidorenko, A.V. Kravtsova, J. Wärnå, A. Aho, I. Heinmaa, I.V. Il'ina , O.V. Ardashov, K.P. Volcho, N.F. Salakhutdinov, D.Yu. Murzin, V.E. Agabekov, Preparation of octahydro-2*H*-chromen-4-ol with analgesic activity from isopulegol and thiophene-2-carbaldehyde in the presence of acid-modified clays, Mol. Catal., 2018, 453, 139–148.

11. K. Zhenz, X. Liu, S. Qin, M. Xie, L. Lin, C. Hu, X. Feng, Completely OH-selective $FeCl_3$-catalyzed Prins cyclization: highly stereoselective synthesis of 4-OH-tetrahydropyrans, *J. Am. Chem. Soc.*, 2012, 134, 17564–17573.

12. J.S. Yadav, B.V. Subba Reddy, A.V. Ganesh, G.G.K.S. Narayana Kumar, $Sc(OTf)_3$-catalyzed one-pot ene-Prins cyclization: a novel synthesis of octahydro-2H-chromen-4-ols, Tetrahedron Lett. 51 (2010) 2963–2966.

13. S. Slater, P.B. Lasonkar, S. Haider, M.J. Alqahtani, A.G. Chittiboyina, I.A. Khan, One-step, stereoselective synthesis of octahydrochromanes via the Prins reaction and their cannabinoid activities, Tetrahedron Tett. 59 (2018) 807–810.

14. P. Borkar, P. van de Weghe, B.V.S Reddy, J.S. Yadav, R. Grée, Unprecedented synergistic effects between weak Lewis and Brønsted acids in Prins cyclization. Chem. Commun., 2012, 48, 9316 – 9318.

15. M. Breugst, R. Grée, K.N. Houk, Synergistic Effects between Lewis and Brønsted Acids: Application to the Prins Cyclization, J. Org. Chem., 2013, 78 (2013) 9892–9897.

16. E. Vyskočilová, A. Gruberová, M. Shamzhy, E. Vrbková, J. Krupka, L. Červený, Prins cyclization in 4-methyl-2-phenyl-tetrahydro-2*H*-pyran-4-ol preparation using smectite clay as catalyst. *Reac. Kinet. Mech. Cat.*, 2018, 124, 711–725.

17. A.O. Zaykovskaya, N. Kumar, E.A. Kholkina, N.S. Li-Zhulanov, P. Maki-Arvela, A. Aho, J. Peltonen, M. Peurla, I. Heinmaa, B.T. Kusema, S. Streiff, D.Yu. Murzin, Synthesis and physico-chemical characterization of Beta zeolite catalysts: Evaluation of catalytic properties in Prins cyclization of (–)-isopulegol, *Micropor. Mesopor. Mat*., 2020, 302, 110236

18. L. Sekerová, E. Vyskočilová, J.S. Fantova, I. Paterová, J. Krupka, L. Červený, Preparation of 2-isobutyl-4-methyltetrahydro-2*H*-pyran-4-ol via Prins cyclization using Fe-modified silica, *Res Chem. Intermed.*, 2017, 43, 4943 – 4958.

19. G.P. More, M. Rane, S.V. Bhat, Efficient Prins cyclization in environmentally benign method using ion exchange resin catalyst, *Green Chem. Lett. and Rev*., 2012, 5, 13 – 17.

20. B.S. Kumar, A. Dhakshinamoorthy, K. Pitchumani, K10 Montmorillonite clays as environmentally benign catalysts for organic reactions, *Catal. Sci. Technol*., 2014, 4, 2378– 2396.

21. O.S. Patrusheva, K.P. Volcho, N.F. Salakhutdinov, Synthesis of oxygen-containing heterocyclic compounds based on monoterpenoids. Russ. Chem. Rev., 2018, 87, 771–796.

22. P. Komadel, Acid activated clays: Materials in continuous demand, *Appl. Clay Sci*., 2016, 131, 84–99.

23. V.A.A. España, B. Sarkar, B. Biswas, R. Rusmin, R. Naidu, Environmental applications of thermally modified and acid activated clay minerals: Current status of the art, *Environ. Technol. Innov.*, 2019, 13, 383 – 397.

24. S. Sadjadi, Halloysite-based hybrids/composites in catalysis, *Appl. Clay Sci*., 2020, 189, 105537.

25. M. Tharmavaram, G.Pandey, D. Rawtani, Surface modified halloysite nanotubes: A flexible interface for biological, environmental and catalytic applications, *Adv. Colloid Interf. Sci.*, 2018, 261, 82 – 101.

26. P. Yuan, D Tan, F. Annabi-Bergaya, Properties and applications of halloysite nanotubes: recent research advances and future prospects, Appl. Clay. Sci., 2015, 112–113, 75–93.

27. S.M. Silva, A.F. Peixoto, C. Freire, HSO_3-functionalized halloysite nanotubes: New acid catalysts for esterification of free fatty acid mixture as hybrid feedstock model for biodiesel production. Appl. Catal. A: Gen., 568, 2018, 221–230.

28. V.M. Abbasov, H.C. Ibrahimov, G.S. Mukhtarova, E. Abdullayev, Acid treated halloysite clay nanotubes as catalyst supports for fuel production by catalytic hydrocracking of heavy crude oil. Fuel, 184, 2016, 555–558.

29. J. Hamdi, A. A. Blanco, B. Diehl, J. B. Wiley, M. L. Trudell, Room-temperature aqueous Suzuki–Miyaura cross-coupling reactions catalyzed via a recyclable palladium@halloysite nanocomposite, Org. Lett., 2019, 21, 10, 3471–3475

30. A. Stavitskaya, K. Mazurova, M. Kotelev, O. Eliseev, P. Gushchin, A. Glotov, R. Kazantsev, V. Vinokurov, Yu. Lvov, Ruthenium-Loaded Halloysite Nanotubes as Mesocatalysts for Fischer–Tropsch Synthesis, *Molecules*, 2020, 25, 1764.

31. A.Yu. Sidorenko, A.V. Kravtsova, A. Aho, I. Heinmaa, H. Pazniak, K.P. Volcho, N.F. Salakhutdinov, D.Yu. Murzin, V.E. Agabekov, Highly selective Prins reaction over acid-modified halloysite nanotubes for synthesis of isopulegol-derived 2H-chromene compounds, *J. Catal*., 2019, 374, 360 – 377.

32. E. Vyskočilová, L. Rezková, E. Vrbková, I. Paterová, L. Červený, Contribution to elucidation of the mechanism of preparation of 2-isobutyl-4-methyltetrahydro-2*H*-pyran-4-ol, Res. Chem. Intermed., 2016, 42, 725–733.

33. A.Yu. Sidorenko, N.S. Li-Zhulanov, P. Mäki-Arvela, T. Sandberg, A.V. Kravtsova, A.F. Peixoto, C. Freire, K.P. Volcho, N.F. Salakhutdinov, V.E. Agabekov, D.Yu. Murzin, Stereoselectivity inversion by water addition in the tandem Prins-Ritter reaction for synthesis of 4-amidotetrahydropyran derivatives, *ChemCatChem*, 2020, 12, 2605–2609.

34. R.A. Sheldon, Green and sustainable manufacture of chemicals from biomass: state of the art, *Green Chem.*, 2014, 16, 950–963.

35. E.P. Barrett, L.G. Joyner, P.P. Halenda, The Determination of Pore Volume and Area Distributions in Porous Substances. *J. Am. Chem. Soc.,* 1951, 73, 373–380.

36. A. Aho, N. Kumar, K. Eränen, T. Salmi, M. Hupa, D.Yu. Murzin, Catalytic pyrolysis of woody biomass in a fluidized bed reactor: Influence of the zeolite structure, *Fuel*, 2008, 87, 2493–2501.

37. A.Yu. Sidorenko, A.V. Kravtsova, A. Aho, I. Heinmaa, T.F. Kuznetsova, D.Yu. Murzin, V.E. Agabekov, Catalytic isomerization of α-pinene oxide in the presence of acid-modified clays, *Mol. Catal.* 2018, 448, 18–29.

38. C.A. Emeis, Determination of Integrated Molar Extinction Coefficients for Infrared absorption bands of pyridine adsorbed on solid acid catalysts, J. Catal., 1993, 141, 347–354.

39. P. Pasbakhsh, G.J. Churchman, J.L. Keeling, Characterisation of properties of various halloysites relevant to their use as nanotubes and microfibre fillers, *Appl. Clay Sci*., 2013, 74, 47–57
40. M. Thommes, K. Kaneko, A.V. Neimark, J.P. Olivier, F. Rodriguez-Reinoso, J. Rouquerol, K.S.W. Sing, Physisorption of Gases, with Special Reference to the Evaluation of Surface Area and Pore Size Distribution (IUPAC Technical Report). *Pure Appl.Chem*., 2015, 87, 1051–1069.
41. E. Abdullayev, A. Joshi, W. Wei, Y. Zhao, Y. Lvov, Enlargement of halloysite clay nanotube lumen by selective etching of aluminum oxide, *ACS Nano*, 2012, 6, 7216 7216–7226.
42. A.F. Peixoto, A.C. Fernandes, C. Pereira, J. Pires, C. Freire, Physicochemical characterization of organosilylated halloysite clay nanotubes, *Micropor. Mesopor. Mat*., 2016, 219, 145 – 154.
43. L. Fu, H. Yang, A. Tang, Y. Hu, Engineering a tubular mesoporous silica nanocontainer with well-preserved clay shell from natural halloysite, Nano Res., 2017, 10, 2782–2799.
44. A. Eschenmoser, J. Diggelmann, D. Felix, US3161657A, 1964.
45. A.Yu. Sidorenko, A.V. Kravtsova, I.V. Il'ina, J. Wärnå, D.V. Korchagina, Yu.V.Gatilov, K.P. Volcho, N.F. Salakhutdinov, D.Yu. Murzin, V.E. Agabekov, Clay nanotubes catalyzed solvent-free synthesis of octahydro-2*H*-chromenols with pharmaceutical potential from (-)-isopulegol and ketones, *J. Catal*, 2019, 380, 145 – 152.
46. J.S. Yadav, B.V. Subba Reddy, G. Mahesh Kumar, C.V.S.R. Murthy, Montmorillonite clay catalyzed in situ Prins–type cyclisation reaction, *Tetrahedron Lett*., 2001, 42, 89–91.
47. R.W. Alder, J.N. Harvey, M.T. Oabley, Aromatic 4-tetrahydropyranyl and 4-tuinuclidinyl tations. Linking Prins with tope and grob, *J. Am. Chem. Soc*., 2002, 124, 4960–4961.
48. D. Murzin, S. Smeds, T. Salmi, Dialkylbenzene hydrogenation: Kinetic analysis of rollover mechanism. *React. Kinet. Catal. Lett*., 1997, 60, 57–64.